

Reprinted from JOURNAL OF APPLIED PHYSICS, Vol. 39, No. 11, 5316-5326, October 1968
 Copyright 1968 by the American Institute of Physics
 Printed in U. S. A.

FEB 21 1969

Pressure and Temperature Dependences of the Isotropic Elastic Moduli of Polycrystalline Alumina

D. H. CHUNG AND GENE SIMMONS

Department of Geology and Geophysics, Massachusetts Institute of Technology, Cambridge, Massachusetts 02139

(Received 25 March 1968; in final form 14 May 1968)

The isotropic elastic moduli of polycrystalline alumina have been determined as a function of hydrostatic pressure up to 10 kbar and also as a function of temperature over the range 4.2° to about 1300°K. The pressure dependence of the elastic moduli is linear over this pressure range. The low-temperature limit of the elastic Debye temperature, 1044 (± 3)°K, compares very well with thermal Debye temperature. Values of various pressure derivatives evaluated at 298°K are as follows:

Pressure derivatives	dL/dp	dG/dp	dB/dp
$(\partial M^*/\partial p)_T$	6.57 (6.58)	1.79 (1.73)	4.19 (4.27)
$(\partial M^T/\partial p)_T$	6.62	1.79	4.23
$(\partial M^*/\partial p)_s$	6.52	1.73	4.16

The quantities in the parentheses are averaged values calculated from the single-crystal second-order elastic constants and their first pressure derivatives. The experimental data are interpreted with respect to (a) the polycrystalline data calculated from the corresponding single-crystal data, (b) the temperature dependence of the isotropic elastic moduli, (c) the acoustic Grüneisen parameters and their comparison with the corresponding quantities evaluated from thermodynamic properties, (d) the equation of state for alumina, and (e) the Debye temperature as a function of temperature and pressure.

1. INTRODUCTION AND THE SCOPE OF THE PRESENT WORK

Precise data for the equation of state for oxides and silicates are important not only because of the direct interest in the basic properties of these materials, but also because such data furnish guidelines for the extrapolation in both temperature and pressure of data for more complex solids (like rocks). As part of a continuing study of the thermodynamic properties of oxides and silicates at high pressure and high temperature, we report in this paper our experimental results on the isotropic elastic parameters of high-purity, high-

density polycrystalline alumina (α -Al₂O₃). The importance of work of this kind has been indicated earlier.^{1,2}

Much experimental work on the thermal and elastic properties of alumina has already been reported: such thermal properties as expansivity^{3,4} and specific heat⁵ are available for high-purity alumina over a wide range of temperature; the single-crystal second-order elastic

¹ G. Simmons, Proc. IEEE **53**, 1337 (1965).

² D. H. Chung, J. Appl. Phys. **38**, 5104 (1967).

³ J. B. Wachtman, Jr. *et al.*, J. Am. Ceram. Soc. **45**, 319 (1962).

⁴ A. Schauer, Can. J. Phys. **43**, 523 (1965).

⁵ G. R. Furukawa *et al.*, J. Res. Natl. Bur. Std. **57**, 67 (1956).

constants^{6,7} and the corresponding polycrystalline isotropic elastic moduli⁸ have been studied carefully over a limited range of temperature (80°–900°K); Bridgman⁹ measured the isothermal volume compressibility and Hart and Drickamer¹⁰ recently extended his values to higher pressure; shock-wave compressions to about 1500 kbar were made by McQueen and Marsh¹¹ on both single-crystal and sintered polycrystalline aluminas; the dependence of sound velocities on hydrostatic pressure¹² to 4 kbar and that on temperature (300°–1400°K)¹³ on a rather "impure" Lucalox alumina¹⁴ was recently reported.

The determination of the third-order elastic constants of this material in both single-crystal¹⁵ and polycrystalline¹⁶ forms has just begun. Our purpose in presenting this paper is to report the isotropic elastic parameters of polycrystalline alumina as a function of hydrostatic pressure to 10 kbar and also as a function of temperature over the range 4.2°–1300°K, and to (1) compare the polycrystalline data with the corresponding single-crystal data, (2) analyze the explicit temperature dependence of the elastic moduli, (3) calculate the acoustic Grüneisen parameters (γ_G and ψ_G) and compare them with the corresponding thermal Grüneisen parameters, (4) give an equation of state for alumina, and (5) calculate the elastic Debye temperature as a function of temperature and pressure.

2. EXPERIMENTAL PROCEDURE

2.1. Specimens and Material Characterization

Several samples of polycrystalline alumina were fabricated by the hot-pressing procedure described by Crandall *et al.*¹⁷ from 99.95% pure α -Al₂O₃ powder. These same specimens were used in earlier measurements⁸ of the isotropic elastic moduli. In the present

study, we used one of the typical samples. It was cut into two pieces—one cube and one rod. The faces of the cube were ground and polished to optically flat and parallel surfaces. The final size of the specimen was 1.28245×1.28143×1.28194 cm. The rod was commercially ground to the shape of a long cylinder to a final size of 0.63501 cm diam × 8.89250 cm in length. The measured density of the specimens was 3.974 g/cm³ at 300°K, which may be compared with the single-crystal density of corundum (3.986 g/cm³). X-ray studies indicate the specimens were made of corundum crystals and inspection of the electron micrograph shows that the grain diameters range from about one to 15 μ .

The elastic isotropy was checked by measuring both the longitudinal and transverse sound velocities in the cube specimen at room conditions for different directions of wave propagation. The specimen was found to be isotropic. The maximum and minimum velocities for the longitudinal wave were 10.848 and 10.842 km/sec. For the transverse wave, the maximum and minimum velocities were 6.379 and 6.375 km/sec, respectively.

The isotropic elastic moduli were determined with McSkimin's pulse-superposition method.¹⁸ X-cut and Y-cut quartz transducers, $\frac{1}{2}$ in. in diameter with fundamental resonance frequencies near 20 MHz, were used.

In general, it is desirable for a bonding material to adhere to both transducer and specimen over the largest temperature and pressure range and accommodate a differential thermal expansivity between transducer and specimen. For this reason, several bonding materials were used as follows: a phenyl-salicylate at room conditions, Dow Corning resin 276-V9 for measurements under hydrostatic pressure, and between 4.2° and 300°K in the ultrasonic method, Fisher's Nonaq stopcock grease. Variations of the isotropic elastic moduli with temperature were determined by a bar-resonance method¹⁹ (above 77°K) and also by the ultrasonic pulse-superposition method¹⁸ (below 300°K).

2.3. Cryostat and High-Temperature Furnace

In the study of temperature dependence using the ultrasonic method, the specimen was mounted on a flat copper plate which was placed in a copper can covered with Styrofoam insulation. A heater coil, a Honeywell germanium resistance thermometer, and a copper-constantan thermocouple were attached to the plate. Three thin brass rods served as supports for the plate and provided a slight thermal contact with the bath of either liquid nitrogen or liquid helium. A Brown electronic recorder was used to control and measure the temperature of the copper plate and the specimen. To ensure that the system had attained thermal equilibrium, a pause of 20–30 min was necessary whenever the

⁶ J. B. Wachtman, Jr. *et al.*, J. Res. Natl. Bur. Std. **64A**, 213 (1960).

⁷ W. E. Tefft, J. Res. Natl. Bur. Std. **70A**, 277 (1966); and also J. B. Wachtman, Jr. *et al.*, Phys. Rev. **122**, 1754 (1961).

⁸ D. H. Chung, Bull. Ceram. Res. **26**, (297), 1 (1961); J. Appl. Phys. **39**, 2777 (1968).

⁹ P. W. Bridgman, Proc. Am. Acad. Arts Sci. **77**, 187 (1949).

¹⁰ H. V. Hart and H. G. Drickamer, J. Chem. Phys. **43**, 2265 (1965).

¹¹ R. G. McQueen, F. Birch, and S. P. Marsh, in *Handbook of Physical Constants*, S. P. Clark, Jr., Ed. (The Geological Society of America, Inc., New York, 1966), p. 154. More recent data were obtained through personal communications (1968).

¹² E. Schreiber and O. L. Anderson, J. Am. Ceram. Soc. **49**, 184 (1966).

¹³ N. Soga, E. Schreiber, and O. L. Anderson, J. Geophys. Res. **71**, 5315 (1966); see also, N. Soga and O. L. Anderson, J. Am. Ceram. Soc. **49**, 355 (1966).

¹⁴ The nature of Lucalox alumina was described by R. L. Coble in U.S. Patent 3,026,210 (Mar. 1962). As described also by S. K. Roy and R. L. Coble, J. Am. Ceram. Soc. **51**, 1 (1968), the Lucalox alumina contains small amounts of magnesium-aluminate spinel as a major secondary phase.

¹⁵ J. H. Gieske (personal communications, 1967).

¹⁶ D. H. Chung (unpublished).

¹⁷ W. B. Crandall *et al.*, in *Mechanical Properties of Engineering Ceramics*, W. Krieger and H. Palmour, Eds. (Interscience Publishers, Inc., New York, 1961).

¹⁸ H. J. McSkimin, J. Acoust. Soc. Am. **37**, 864 (1965).

¹⁹ S. Spinner and W. E. Tefft, Proc. ASTM **61**, 1221 (1961).

temperature was changed. The thermocouple was used for measuring temperatures above 77°K and the resistance thermometer below. The resistance-temperature characteristics of the germanium thermometer were taken from the Honeywell calibration tables for the thermometer. Over the temperature range below 77°K, the temperature was measured to better than 0.5 deg and was controlled to at least one degree over the time required for a measurement.

The cryostat assembly used for determinations of the elastic moduli using the resonance method consisted of a specimen chamber, heater, and support placed in an insulated Dewar. The specimen chamber was made of copper and placed directly against the upper end of a Kanthol wound heater. Both the specimen chamber and the heater were supported by a brass fitting set on the bottom of a stainless steel Dewar-flask (Hoffman model S/N 210-22). The assembly was immersed in a liquid-nitrogen bath to make the measurement at 77°K. Temperature of the specimen chamber was controlled by a variac and readings were taken by setting the variac and allowing a sufficient time for thermal equilibrium to be approached closely. The time interval allowed for this purpose varied from 30 min to about two hours. Over the temperature range 77°–300°K, a copper-constantan thermocouple (which had been calibrated previously against an NBS standard) was used to measure the specimen temperature. A frosting of water vapor on the specimen surface was prevented by a constant flow of precooled N₂ gas. The specimen temperature was kept constant within 1 deg during the time required for measurements.

Measurements of resonant frequencies as a function of temperature above 300°K were made in a Kanthol wound tube-furnace connected to a variac. The upper temperature limit of the furnace was about 1330°K. The specimen temperature was measured with a platinum-platinum plus 10% rhodium thermocouple which had been calibrated earlier against an NBS standard, and was recorded with an accuracy better than ± 3 deg.

2.4. Hydrostatic Pressure System

The equipment used for the generation of hydrostatic pressure was constructed by the Harwood Engineering Company, Walpole, Mass. The unit was designed for the production of hydrostatic pressures to about 14 kbar. Argon gas was the pressure medium. The pressure was measured with a manganin cell in connection with a Foxboro Dynalog recorder. The temperature of the sample was kept constant by the circulation of warm water outside of the entire pressure cell. The temperature of a copper plate which was in direct contact with one of the specimen faces was measured with a chromel-alumel thermocouple. With another thermocouple, the temperature was measured on the opposite face of the specimen to guard against the presence of thermal gradients within the specimen. In each determination,

the frequency was recorded only after ascertaining the system had reached thermal equilibrium; usually, a wait of 15–20 min after changing pressure was sufficient for this purpose.

3. EXPERIMENTAL RESULTS

3.1. Variation of the Isotropic Elastic Moduli with Pressure

The quantity of interest in our pressure experiments is the first derivative of an elastic modulus M with respect to hydrostatic pressure evaluated at zero-pressure, $(dM/dp)_{p=0}$. This derivative is an isothermal one. For a modulus M , we have

$$M = 4\rho l^2 f^2, \quad (3.1)$$

where f is the corrected repetition frequency. Taking logarithms and differentiating both sides with respect to pressure,

$$d(\ln M)/dp = d(\ln \rho)/dp + 2[d(\ln l)/dp] + d(\ln f^2)/dp. \quad (3.2)$$

Since $(d \ln l / dp) = (d \ln V / dp) / 3$ in our case, and $(d \ln \rho / dp) = -(d \ln V / dp)$, where V is volume, and after evaluating the derivatives at $p = 0$, we have

$$[d(\ln M)/dp]_{p=0} = (1/3B^T)_{p=0} + [(d/dp)(f/f_0)^2]_{p=0} \quad (3.3)$$

or

$$(dM/dp)_{p=0} = (M/3B^T)_{p=0} + [M \cdot (d/dp)(f/f_0)^2]_{p=0}. \quad (3.4)$$

B^T is the isothermal bulk modulus and it is related to the adiabatic bulk modulus B^s by $B^T = B^s(1 + T\beta\gamma_G)^{-1}$, where β is the coefficient of volume expansion, γ_G is Grüneisen's ratio, and T is temperature in °K.

Table I summarizes the isotropic elastic properties of the specimen at 298°K along with the corresponding quantities evaluated for nonporous polycrystalline aluminas. Table II is a listing of the relative change in the linear dimension of the specimen, the ratio of the frequency squared, and density as a function of hydrostatic pressure up to 10 kbar. The values of (l/l_0) were found according to Cook's approximation scheme.²⁰ The corresponding density values were calculated from $\rho = \rho_0(l_0/l)^3$, where ρ_0 is the initial density of the specimen. The sound velocities at a given pressure p were then calculated according to $v_j = v_{j(0)}(f_j/f_{j(0)})(l/l_0)$, where the subscript (0) denotes the quantity at the unstrained condition; the isotropic elastic moduli were then calculated in the usual way.

The first pressure derivatives of sound velocities at 298°K were found as follows: $(dv_l/dp) = 5.35$ and $(dv_t/dp) = 2.20$ in units of 10^{-3} (km/sec)/kbar. The

²⁰ R. K. Cook, J. Acoust. Soc. Am. 29, 445 (1957).

TABLE I. Density, sound velocities, and isotropic elastic moduli of the alumina specimen and the corresponding quantities evaluated at the single-crystal density-point (at 298°K).

Quantity	Measured values	Values ^b corrected for porosity
Density (g/cm ³)	3.974	3.986
Longitudinal velocity (km/sec)	10.845(±0.003) ^a	10.889
Transverse velocity (km/sec)	6.377(±0.002) ^a	6.398
Adiabatic longitudinal modulus (×10 ¹¹ dyn/cm ²)	46.739	47.262
Shear modulus (×10 ¹¹ dyn/cm ²)	16.160	16.316
Adiabatic bulk modulus (×10 ¹¹ dyn/cm ²)	25.192	25.507
Isothermal bulk modulus (×10 ¹¹ dyn/cm ²)	25.033	25.346

^a These variations in sound velocities represent the observed variations in the velocities when the direction of wave propagation was changed. Since these variations were less than the expected experimental error, the specimen was considered elastically isotropic (see text for the description).

^b Values obtained from Ref. 8.

corresponding derivatives of the isotropic elastic moduli were: from Eq. (3.4), $(dL^s/dp) = 6.51$, $(dG/dp) = 1.77$, and $(dB^s/dp) = 4.16$ calculated from the former, whereas using Cook's method, 6.5, 1.8 and 4.2, respectively. These values may be compared with the cor-

TABLE II. The relative change in the linear dimension, ratio of the frequency squared, and density as a function of hydrostatic pressure (at 298°K).

Pressure (kbar)	(l/l_0)	Density (g/cm ³)	$(f_i/f_{i(0)})^2$	$(f_t/f_{t(0)})^2$
0.001	1.000000	3.974	1.00000	1.00000
1.0	0.999867	3.976	1.00127	1.00097
2.0	0.999735	3.977	1.00252	1.00193
3.0	0.999603	3.979	1.00378	1.00289
4.0	0.999470	3.980	1.00504	1.00385
5.0	0.999338	3.982	1.00630	1.00481
6.0	0.999206	3.984	1.00757	1.00577
7.0	0.999076	3.985	1.00882	1.00673
8.0	0.998943	3.987	1.01008	1.00769
9.0	0.998811	3.988	1.01135	1.00865
10.0	0.998682	3.990	1.01260	1.00960

responding quantities obtained on a Lucalox alumina specimen by Schreiber and Anderson.¹² Their values were: $(dL^s/dp) = 6.34$, $(dG/dp) = 1.75$, and $(dB^s/dp) = 3.98$ at 298°K.

3.2. Variation of the Isotropic Elastic Parameters with Temperature

Figures 1 and 2 are plots of sound velocities as a function of temperature. The data points below 300°K consist of two kinds: one, velocities resulting directly

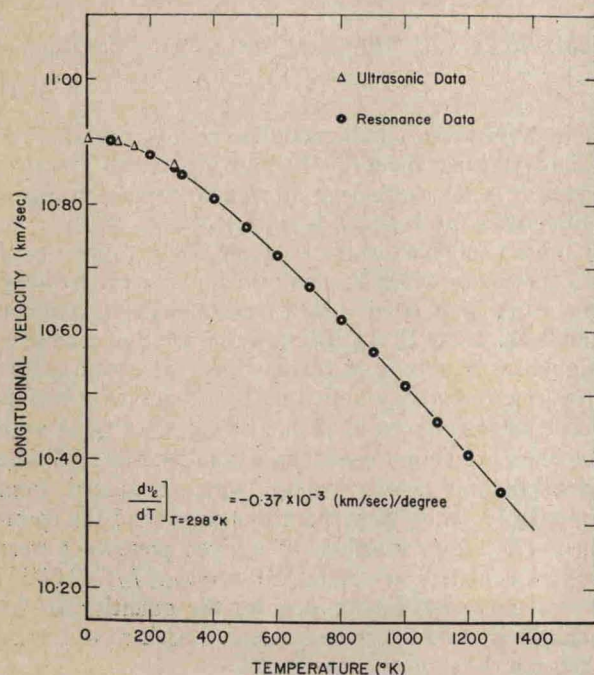


FIG. 1. Temperature dependence of the longitudinal sound velocity determined on a polycrystalline alumina specimen of $\rho_0 = 3.974$ g/cm³. Data points consist of two kinds: one, velocities resulting directly from the ultrasonic method and the other, velocities calculated from the density and measured isotropic elastic moduli resulting from the bar-resonant method.

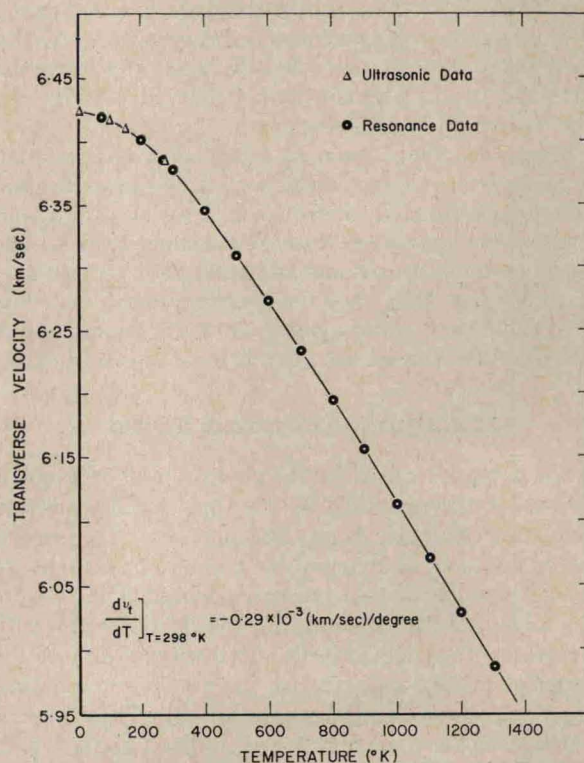


FIG. 2. Temperature dependence of the transverse sound velocity determined on a polycrystalline alumina specimen of $\rho_0 = 3.974$ g/cm³. Data points consist of two kinds: one, velocities resulting directly from the ultrasonic method and the other, velocities calculated from the density and measured shear modulus resulting from the bar-resonant method.

TABLE III. Acoustic data for polycrystalline α -Al₂O₃ (at 298°K).

Pressure (kbar)	Density (g/cm ³)	Sound velocities			Elastic moduli			$\theta_{D(\text{elastic})}$ (°K)
		v_l	v_t (km/sec)	v_m	L^*	G ($\times 10^{11}$ dyn/cm ²)	B^*	
0.001	3.986	10.889	6.398	7.092	47.262	16.316	25.507	1034.9
1.0	3.988	10.894	6.400	7.094	47.333	16.335	25.552	1035.4
2.0	3.989	10.900	6.402	7.097	47.391	16.351	25.590	1035.8
3.0	3.991	10.905	6.404	7.099	47.461	16.370	25.635	1036.4
4.0	3.992	10.910	6.407	7.102	47.520	16.385	25.672	1036.8
5.0	3.994	10.916	6.409	7.104	47.590	16.404	25.718	1037.4
6.0	3.996	10.921	6.411	7.107	47.660	16.424	25.762	1037.9
7.0	3.997	10.927	6.413	7.109	47.720	16.439	25.800	1038.4
8.0	3.999	10.932	6.415	7.112	47.790	16.458	25.845	1038.9
9.0	4.000	10.937	6.418	7.114	47.848	16.474	25.883	1039.4
10.0	4.002	10.943	6.420	7.117	47.919	16.494	25.928	1039.9

from the ultrasonic method and the other, calculated velocities from the measured moduli resulting from the resonant method. Above 300°K, all values of the sound velocities were calculated from measured isotropic elastic moduli and density evaluated at a given temperature.

At 298°K, the isotropic temperature derivatives of sound velocities were: $(dv_l/dT) = -0.37(\pm 0.022)$ and $(dv_t/dT) = -0.29(\pm 0.016)$ in units of 10^{-3} (km/sec)/deg. The corresponding derivatives of the isotropic elastic moduli at 298°K were found as: $(dL^*/dT) = -0.39(\pm 0.030)$, $(dG/dT) = -0.16(\pm 0.014)$, and $(dB^*/dT) = -0.17$ in units of 10^9 (dyn/cm²)/deg. At 1000°K, however, the corresponding derivatives were as follows: $(dv_l/dT) = -0.53$ and $(dv_t/dT) = -0.41$ in units of 10^{-3} (km/sec)/deg, and $(dL^*/dT) = -0.55(\pm 0.026)$, $(dG/dT) = -0.23(\pm 0.020)$ and $(dB^*/dT) = -0.24$ in units of 10^9 (dyn/cm²)/deg.

Comparing the present data with the similar data available for a Lucalox alumina,¹³ we note the following: our values of the adiabatic bulk modulus, for example, at 298°K and also at 1000°K are 25.51 and 23.95 in units of 10^{11} dyn/cm², respectively, whereas the Lucalox data¹³ were 24.87 and 23.19 in the same units. The apparent differences of about 3% are beyond the limits of the expected experimental errors in both cases, and these may be associated with the foreign materials contained in the Lucalox specimen.

4. DATA ANALYSIS AND COMPARISON OF POLYCRYSTALLINE DATA WITH THE CORRESPONDING SINGLE-CRYSTAL DATA

A realistic test of the correspondence between the single-crystal acoustic data and polycrystalline acoustic data demands essentially three general requirements: (a) the representative set of the single-crystal acoustic data, (b) the polycrystalline acoustic data evaluated for the corresponding density, and (c) an averaging

scheme by which the anisotropic single-crystal acoustic data can be converted into isotropic acoustic data. The requirement (c) has been considered in Ref. 2. The requirement (a) can be met by considering the recent data on the single-crystal elastic constants as a function of temperature⁷ as well as a function of pressure.¹⁵ In this section, on the basis of the experimental results presented in Sec. 3, polycrystalline acoustic data corresponding to the single-crystal density are evaluated and compared with isotropic properties calculated from the single-crystal data.

4.1. Variation with Pressure

In the first-order approximation for low porosities, the porosity-dependent elastic modulus M is given by^{21,22}

$$M = M_0(1 - \alpha\eta), \quad (4.1)$$

where M_0 is the elastic modulus of nonporous materials and η is the porosity. α is a constant. Differentiating Eq. (4.1) with respect to pressure, we find

$$dM/dp = (dM_0/dp)(1 - \alpha\eta) - M_0\alpha(d\eta/dp). \quad (4.2)$$

Because the rate of change of porosity with pressure $(d\eta/dp)$ in our specimen is estimated to be -3×10^{-6} /kbar, the last term can be ignored and we obtain

$$(1/M)(dM/dp) = (1/M_0)(dM_0/dp). \quad (4.3)$$

The physical implication of Eq. (4.3) is that the pressure coefficient of an elastic modulus determined on porous polycrystalline aggregate represents the corresponding quantity of the nonporous polycrystalline aggregates. A departure from Eq. (4.3), if observed, would then correspond to effects of the $(\alpha\eta)$ term.

On the basis of Eq. (4.3) and experimental results

²¹ For a review, see N. A. Weil, in *High Temperature Technology* (Butterworths Scientific Publications Inc., Washington, D.C., 1964), p. 217.

²² J. B. Walsh, *J. Geophys. Res.* **70**, 381 (1965).

TABLE IV. Single-crystal elastic constants and their first pressure derivatives for trigonal α -Al₂O₃ (at 298°K).^a

Index for elastic constants	11	33	44	66	12	13	14
$c_{\mu\nu}$ ($\times 10^{11}$ dyn/cm ²)	49.781	50.192	14.752	16.751	16.279	11.735	-2.286
$(dc_{\mu\nu}/dp)_{T=298^\circ\text{K}}$	6.14	5.03	2.24	1.44	3.26	3.67	0.164

^a J. H. Gieske (private communications).

presented in Tables I and II, we find from the use of Eq. (3.4) that $(dL^*/dp)=6.57$, $(dG/dp)=1.79$, and $(dB^*/dp)=4.19$. These values represent the first pressure derivatives of the isotropic elastic moduli (evaluated at $p=0$) for the nonporous aggregates of polycrystalline alumina and these are to be compared with the corresponding quantities calculated from the single-crystal data. Table III is a tabulation of the density, sound velocities, and isotropic elastic moduli as a function of hydrostatic pressure. Also entered here are the computed *mean* velocity of sound and the Debye temperature of which a discussion follows later in Sec. 5.

The single-crystal second-order elastic constants and their pressure dependence up to about 10 kbar have been determined recently by Gieske.¹⁵ Gieske's results¹⁵ at 298°K are reproduced in Table IV. Using these single-crystal data, the pressure derivatives of the isotropic elastic moduli were calculated.

The first pressure derivatives of the isotropic polycrystalline elastic moduli in terms of the corresponding single-crystal properties are²

$$B^* = (B_V' + B_R')/2 \quad (4.4)$$

and

$$G^* = (G_V' + G_R')/2, \quad (4.5)$$

where

$$B_V' = [2(c_{11}' + c_{12}') + c_{33}' + 4c_{13}']/9 \quad (4.6)$$

$$B_R' = C_b(B_R/C_c)^2 C_c' - (B_R^2/C_c) C_b' \quad (4.7)$$

$$G_V' = (C_b' + 12c_{44}' + 12c_{66}')/30, \quad (4.8)$$

and

$$G_R' = [6B_V(G_R/C_c)^2 C_c' - 6(G_R^2/C_c) B_V' + 4(G_R/C_h)^2 C_h' - 4(G_R^2/C_h) c_{44}' + 2C_a(G_R/C_h)^2 C_h' - 2(G_R^2/C_h) C_a']/5, \quad (4.9)$$

where

$$C_a = c_{11} - c_{12} \quad \text{and} \quad C_a' = c_{11}' - c_{12}' \quad (4.10)$$

$$C_b = c_{11} + c_{12} + 2c_{33} - 4c_{13}$$

and

$$C_b' = c_{11}' + c_{12}' + 2c_{33}' - 4c_{13}' \quad (4.11)$$

$$C_c = c_{33}(c_{11} + c_{12}) - 2c_{13}^2$$

and

$$C_c' = (c_{11} + c_{12})c_{33}' + c_{33}(c_{11}' + c_{12}') - 4c_{13}c_{13}' \quad (4.12)$$

$$C_h = C_a c_{44} - 2c_{14}^2$$

and

$$C_h' = C_a c_{44}' + c_{44} C_a' - 4c_{14}c_{14}' \quad (4.13)$$

$$B_V = [2(c_{11} + c_{12}) + c_{33} + 4c_{13}]/9 \quad (4.14)$$

$$B_R = [c_{33}(c_{11} + c_{12}) - 2c_{13}^2]/(c_{11} + c_{12} + 2c_{33} - 4c_{13}) \quad (4.15)$$

$$G_R = (5/2) \{ (C_a c_{44} c_{66}) / [C_c (c_{44} + c_{66}) + 3B_V c_{44} c_{66}] \} \quad (4.16)$$

and the primes denote the first pressure derivatives. From B^* and G^* from Eqs. (4.4) and (4.5), the pressure derivative of the isotropic longitudinal modulus L^* can be found as

$$L^* = B^* + 4G^*/3. \quad (4.17)$$

The calculated values for B^* , G^* , and L^* are compared with the polycrystalline acoustic data in Table V. Also entered in the table are the limiting values. It is noted that the calculated and experimental values compare very well.

Using the procedure outlined in Ref. 2, the isothermal pressure derivatives of the adiabatic elastic moduli have been converted into (i) isothermal pressure derivatives of the isothermal elastic moduli and (ii) the adiabatic pressure derivatives of the adiabatic elastic moduli; the results are summarized in Table VI. In

TABLE V. Comparison of predicted and experimental isotropic pressure derivatives of polycrystalline elastic moduli for trigonal α -Al₂O₃ (at 298°K).

Pressure derivatives	Density (g/cm ³)	dB/dp			dG/dp			dL/dp		
		(dB_V/dp)	(dB_R/dp)	(dB^*/dp)	(dG_V/dp)	(dG_R/dp)	(dG^*/dp)	(dL_V/dp)	(dL_R/dp)	(dL^*/dp)
Predicted ^a	3.986	4.28	4.26	4.27	1.63	1.83	1.73	6.45	6.70	6.58
Experimental	3.986	4.19	1.79	6.57

^a Calculated from the single-crystal acoustic data.

TABLE VI. Pressure derivatives of polycrystalline elastic moduli at different thermodynamic boundary conditions (at 298°K).

Pressure derivatives	dB/dp	dG/dp	dL/dp
$(\partial M^s/\partial p)_T$	4.19 ^a 3.70 ^b	1.79 ^a	6.57 ^a
$(\partial M^T/\partial p)_T$	4.23 4.10 ^c	1.79	6.62
$(\partial M^s/\partial p)_s$	4.16	1.73	6.52

^a These are taken from Table V.^b This is calculated from the Dugdale-MacDonald relation, i.e., $(\partial B^s/\partial p)_T = 2\gamma_G + 1$, where γ_G is the Grüneisen parameter.^c This was obtained from the Murnaghan equation of state by a curve-fitting procedure using experimental data on compression.

Table VI, two other values of pressure derivative of the bulk modulus have been listed. One is a theoretical value based on the Dugdale-MacDonald relation,²³ and the other is derived from the Murnaghan equation of state²⁴ by a curve-fitting procedure using experimental data on compression.⁹⁻¹¹ A detailed discussion on these quantities will follow in Sec. 5. It is seen, however, that these values compare reasonably well with the corresponding quantities resulting from the ultrasonic-pressure experiments made on both the single-crystal and polycrystalline materials.

4.2. Variation with Temperature

Recalling Eq. (4.1), the temperature derivative of the porosity-sensitive elastic modulus is

$$dM/dT = (dM_0/dT)(1 - \alpha\eta) - M_0\alpha(d\eta/dT). \quad (4.18)$$

Since $(d\eta/dT)$ is zero, the last term drops out. Thus, dividing the resulting part of Eq. (4.18) by Eq. (4.1), we obtain

$$(1/M)(dM/dT) = (1/M_0)(dM_0/dT). \quad (4.19)$$

Equation (4.19) implies that the temperature coefficient of an elastic modulus determined on a porous polycrystalline specimen can be used to estimate the elastic modulus of the nonporous polycrystalline aggregates (as a function of temperature) simply by interpolating the room-temperature modulus of the porous aggregate to that of the nonporous aggregate. The result of such interpolations is given in Table VII. This represents the isotropic elastic parameters of polycrystalline alumina as a function of temperature, which are to be compared with the corresponding single-crystal data.

²³ J. S. Dugdale and D. K. C. MacDonald, Phys. Rev. **89**, 832 (1953).

²⁴ F. D. Murnaghan, Proc. Natl. Acad. Sci. **30**, 244 (1944); F. D. Murnaghan, *Non-Linear Problems in Mechanics of Continua, Proceedings of the Symposium on Applied Mathematics* (American Mathematical Society, Providence, R.I., 1949) Vol. 1.

Figure 3 illustrates the comparison of polycrystalline longitudinal modulus with the corresponding quantity calculated from the single-crystal data using the Voigt-Reuss-Hill (VRH) approximation. The single-crystal data used here are those of Tefft.⁷ Figure 4 is a similar comparison for the isotropic shear modulus. It is evident that the comparison is good for the shear modulus throughout the temperature range considered. For the longitudinal modulus, we note that there is a significant discrepancy between our data and the VRH modulus calculated from Tefft's single-crystal data (particularly at low temperatures). At present, it is very difficult to see why the longitudinal modulus at temperatures below 100°K calculated from the single-crystal data decreases with decreasing temperature. Our measurements on polycrystalline specimens indicate exactly the opposite behavior so that the elastic moduli become *stiffer* as temperature decreases.

5. INTERPRETATION AND DISCUSSION

5.1. Analysis of Temperature Dependence of the Isotropic Elastic Moduli

The total temperature dependence of an elastic modulus can be thought of as consisting of two parts: one, a result of an explicit temperature change, and the other an implicit part resulting from a change in volume with temperature. In other words, the elastic modulus

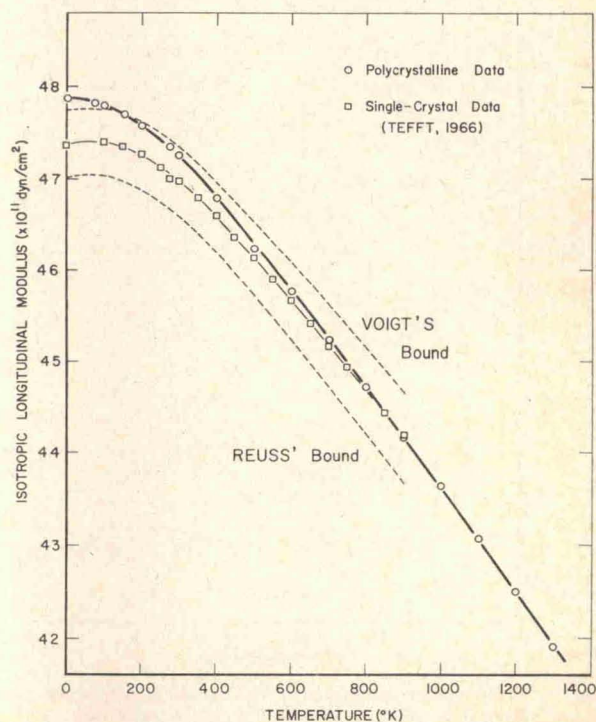


FIG. 3. A comparison between the measured and calculated isotropic longitudinal modulus as a function of temperature.

TABLE VII. Thermo-elastic properties of polycrystalline α - Al_2O_3 (at 1 atm).

Temperature (°K)	Density (g/cm ³)	Velocities			Elastic moduli			$\theta_{D(\text{elastic})}$ (°K)
		v_l	v_t (km/sec)	v_m	L^s ($\times 10^{11}$ dyn/cm ²)	B^s		
4.2	3.9924	10.951	6.448	7.146	47.879	16.599	25.747	1044(±3)
77	3.9920	10.947	6.446	7.144	47.839	16.587	25.727	1043
100	3.9918	10.942	6.444	7.141	47.793	16.576	25.691	1042.6
150	3.9910	10.931	6.437	7.134	47.687	16.537	25.638	1041
200	3.9896	10.919	6.427	7.123	47.566	16.480	25.593	1040
273	3.9863	10.896	6.408	7.102	47.326	16.369	25.512	1036
300	3.986	10.889	6.398	7.092	47.262	16.362	25.507	1035
400	3.978	10.844	6.368	7.059	46.778	16.131	25.270	1029
500	3.969	10.798	6.333	7.021	46.277	15.918	25.053	1023
600	3.960	10.750	6.296	6.981	45.763	15.697	24.833	1016
700	3.949	10.702	6.259	6.941	45.229	15.470	24.602	1010
800	3.939	10.653	6.218	6.896	44.702	15.230	24.396	1002
900	3.928	10.602	6.178	6.853	44.152	14.992	24.162	995
1000	3.918	10.552	6.137	6.809	43.625	14.756	23.950	988
1100	3.907	10.498	6.096	6.764	43.058	14.519	23.700	981
1200	3.897	10.444	6.053	6.718	42.507	14.278	23.470	972
1300	3.886	10.386	6.011	6.667	41.918	14.041	23.197	965

M of Born-von Karman-type solids can be treated as a function of volume V (interatomic separation) and temperature T ²⁵:

$$M = M(V, T). \quad (5.1)$$

Taking logarithms and differentiating both sides with

respect to pressure, and rearranging the results, we find

$$d(\ln M)/dT = -\beta B^T [\partial(\ln M)/\partial p]_T + [\partial(\ln M)/\partial T]_V, \quad (5.2)$$

where B^T is the isothermal bulk modulus. Hence, from our data on both the pressure and temperature dependences of the isotropic elastic moduli, we should be able to separate out the *changes* due to temperature from those due to volume. Rewriting Eq. (5.2) for the explicit term

$$[\partial(\ln M)/\partial T]_V = d(\ln M)/dT + \beta B^T [\partial(\ln M)/\partial p]_T. \quad (5.3)$$

(explicit) = (total) + (implicit).

In Table VIII, both the pressure and temperature coefficients of longitudinal, shear, and bulk moduli evaluated at zero-pressure and 298°K are listed. The quantities of our interest $(\partial \ln M/\partial T)_V$, found from these values, are entered in the last column. Any assumption that an elastic modulus is a unique function

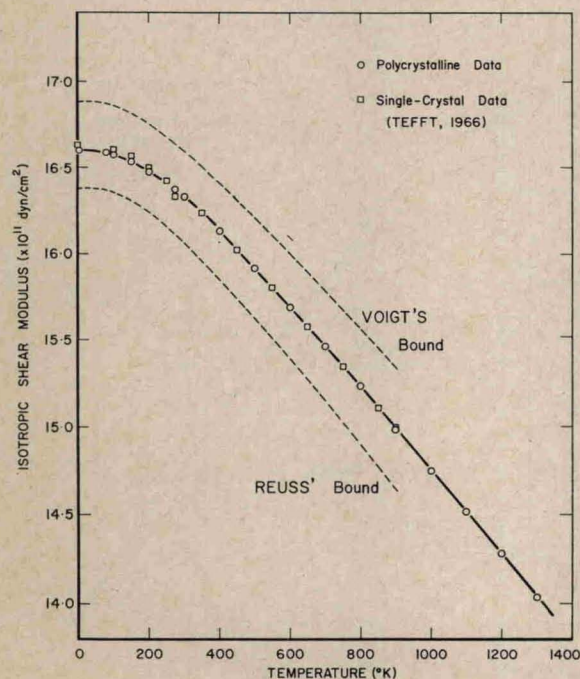


FIG. 4. A comparison between the measured and calculated isotropic shear modulus as a function of temperature.

TABLE VIII. Pressure and temperature coefficients of the adiabatic elastic moduli of polycrystalline α - Al_2O_3 (at 298°K).

Adiabatic elastic modulus	$d(\ln M)/dT$ ($\times 10^{-5}/^\circ\text{K}$)	$\beta B^T [\partial(\ln M)/\partial p]_T^a$ ($\times 10^{-5}/^\circ\text{K}$)	$[\partial(\ln M)/\partial T]_V$ ($\times 10^{-5}/^\circ\text{K}$)
L^s	-8.23	+5.56	-2.67
G	-9.79	+4.45	-5.34
B^s	-6.664	+6.658	-0.006

^a Based on Eq. (5.3), where $\beta = 1.641 \times 10^{-5}/^\circ\text{K}$ and $B^T = 25.346 \times 10^{11}$ dyn/cm².

²⁵ D. Lazarus, Phys. Rev. **76**, 545 (1949).

TABLE IX. Thermal Grüneisen's first and second parameters for α -Al₂O₃.

Temperature (°K)	β ($\times 10^{-6}/^\circ\text{K}$)	C_p (cal/mol·°K)	V (cm ³ /mol)	B^* ($\times 10^{11}$ dyn/cm ²)	$\gamma_{G(\text{thermal})}$	(1+ $T\beta\gamma_G$)
4.2	?	0.0021	25.538	25.747
77	1.08	1.50	25.539	25.727	1.13	1.000094
100	2.40	3.07	25.540	25.691	1.23	1.000294
150	6.15	7.64	25.545	25.638	1.26	1.001162
200	10.23	12.22	25.555	25.593	1.31	1.002677
273	14.88	17.482	25.578	25.512	1.33	1.005389
298	16.41	18.98	25.580	25.507	1.35	1.006636
400	20.10	23.38	25.631	25.270	1.33	1.010698
500	22.05	25.55	25.689	25.053	1.33	1.014632
600	23.55	26.85	25.748	24.833	1.34	1.018935
700	24.69	27.75	25.820	24.602	1.35	1.023340
800	25.65	28.44	25.885	24.396	1.36	1.027926
900	26.55	28.99	25.950	24.162	1.37	1.032787
1000	27.42	29.47	25.022	23.950	1.39	1.037993
1100	28.14	29.90	26.097	23.700	1.39	1.043054
1200	28.68	30.29	26.164	23.470	1.39	1.047815
1300	29.34	30.66	26.235	23.197	1.39	1.053077

of volume is evidently invalid (especially in the case of the longitudinal and shear moduli), since the last term in Eq. (5.2) vanishes if $M = M(V)$.

5.2. Grüneisen's Parameters and Equation of State for Alumina

Essentially, there are two Grüneisen's parameters; one given by

$$\gamma_G = \beta V / C_p \chi^* = \beta V B^* / C_p = \gamma_{G(\text{thermal})} \quad (5.4)$$

and the other

$$\begin{aligned} \psi_G &= -[\partial(\ln B^*) / \partial T / \partial(\ln V) / \partial T]_p \\ &= -(1/\beta B^*) (\partial B^* / \partial T)_p = \psi_{G(\text{thermal})}, \end{aligned} \quad (5.5)$$

where β is the coefficient of volume thermal expansion, V is the volume, B^* is the adiabatic bulk modulus, C_p is the specific heat at constant pressure, and χ^* is the adiabatic compressibility. These parameters give a measure of the anharmonicity of the interatomic potential, and they are useful in the study of the solid equation of state.²⁶⁻³⁰ In Table IX, these parameters are tabulated as a function of temperature. The data on thermal expansion are due to Wachtman *et al.*³ and Schauer.⁴ The data on specific heats were taken from tables presented by the National Bureau of Standards.⁵

²⁶ E. Grüneisen, in *Handbuch der Physik*, H. Geiger and K. Scheel, Eds. (Springer-Verlag, Berlin, 1926), Vol. X, Pt. I. For an English translation, see NASA Tech. Rept. No. RE2-18-59W (Feb. 1959).

²⁷ J. C. Slater, *Introduction to Chemical Physics* (McGraw-Hill Book Co., New York, 1939).

²⁸ F. Birch, *Phys. Rev.* **71**, 809 (1947); *J. Geophys. Res.* **57**, 227 (1952).

²⁹ T. H. K. Barron, *Phil. Mag.* **7**(46), 720 (1955); *Ann. Phys.* (New York) **1**, 77 (1957).

³⁰ J. J. Gilvarry, *J. Appl. Phys.* **28**, 1253 (1957); *J. Appl. Phys.* **33**, 3595 (1962).

It is seen here that the first Grüneisen parameter, often termed Grüneisen's ratio, remains almost constant with temperature above 200°K (which is about $0.2\theta_D$). This constancy supports the Grüneisen theory of solids.

The parameters defined by Eqs. (5.4) and (5.5) are *thermal* Grüneisen's ratio and *thermal* Grüneisen's anharmonic parameter, respectively, and it can be shown easily that they are related to the pressure derivatives of the elastic moduli. The relationship between γ_G and (dB/dp) , with two simplifying assumptions,²⁷ was given first by Slater. The Slater relation²⁷ is

$$\gamma_{\text{Slater}} = \frac{1}{2} (\partial B^* / \partial p)_T - \frac{1}{6} \quad (5.6)$$

and from our data $\gamma_{\text{Slater}} = 1.95$. The general relationship between γ_G and (dM/dp) is based on a correspondence relation that, within the quasiharmonic approximation,²⁹

$$\gamma_{G(\text{thermal})} = \gamma_{G(\text{acoustic})}, \quad (5.7)$$

where

$$\gamma_{G(\text{acoustic})} = \sum \gamma_i C_i(\nu_i) / \sum C_i(\nu_i), \quad (5.8)$$

where

$$\gamma_i = -d(\ln \nu_i) / d(\ln V), \quad (5.9)$$

and $C_i(\nu_i)$ are Einstein's specific heats of the i th mode having the frequency ν_i . In terms of the single-crystal elastic constants and their first pressure derivatives, Smith and his collaborators³¹ presented the corresponding expression for Eq. (5.9). For isotropic solids (like a strain-free glass and a polycrystalline aggregate), the equivalent expression for Eq. (5.9) is

$$\bar{\gamma}_j = -\frac{1}{6} + (B^*/2) (\partial \ln M_j^* / \partial p)_T, \quad (5.10)$$

³¹ C. S. Smith, D. E. Schuele, and W. B. Daniels, in *Physics of Solids at High Pressures*, C. T. Tomizuka and R. M. Emrick, Eds. (Academic Press Inc., New York, 1965). See also D. E. Schuele and C. S. Smith, *J. Phys. Chem. Solids* **25**, 801 (1964).

where the subscript j refers to either longitudinal or transverse modes so that

$$\bar{\gamma}_l = -\frac{1}{6} + (B^T/2L^s)(\partial L^s/\partial p)_T \quad (5.11)$$

and

$$\bar{\gamma}_t = -\frac{1}{6} + (B^T/2G)(\partial G/\partial p)_T. \quad (5.12)$$

The bar over the gammas indicates $\bar{\gamma}_j = \gamma_j(\phi, \theta)$, and these $\bar{\gamma}_j$ are *isotropic*. The physical implication of Eqs. (5.11) and (5.12) is that there are acoustic longitudinal modes with the longitudinal velocity v_l and a corresponding longitudinal Grüneisen mode-gamma $\bar{\gamma}_l$, and acoustic transverse modes with transverse velocity v_t and a corresponding Grüneisen mode-gamma $\bar{\gamma}_t$.³¹ Thus, the *total* Grüneisen parameter $\bar{\gamma}$ is given by (as T approaches zero)

$$\bar{\gamma} = (\bar{\gamma}_l/3)(v_m/v_l)^3 + (2\bar{\gamma}_t/3)(v_m/v_t)^3 = \bar{\gamma}_0. \quad (5.13)$$

At high temperatures, we find a similar expression to that of Smith *et al.*³¹ to be

$$\bar{\gamma}_\infty = \frac{1}{3}(\bar{\gamma}_l + 2\bar{\gamma}_t). \quad (5.14)$$

However, it is noted that since at high temperatures the optical and short-wave acoustic modes are excited the mode-gammas corresponding to these vibrations will be affected by these modes. Equation (5.14) does not take into account these modes; therefore, $\bar{\gamma}_\infty$ obtained by Eq. (5.14) will not give the exact value of the high-temperature limit of the Grüneisen parameter, but instead it gives an approximate value which is accurate only in a first-order approximation.

Using our acoustic data, the calculated mode-gammas are as follows: $\bar{\gamma}_l = 1.58$ and $\bar{\gamma}_t = 1.22$. And the limiting values are: $\bar{\gamma}_0 = 1.26$ and $\bar{\gamma}_\infty = 1.58$, and these may be compared with $\gamma_{G(\text{thermal})}$ tabulated in Table IX.

The second Grüneisen parameter $\psi_{G(\text{thermal})}$ can be found from the acoustic data also. It has been shown by Birch^{28,32} that

$$-(1/\beta B^T)(\partial B^T/\partial T)_p = (\partial B^T/\partial p)_T = \psi'_{G(\text{acoustic})}, \quad (5.15)$$

where

$$(\partial B^T/\partial p)_T = (\partial B^s/\partial p)_T + C = \psi_{G(\text{acoustic})}. \quad (5.16)$$

The dimensionless constant C is given by Overton's relation²

$$\begin{aligned} -C = & [(A-1)/A][(2/\beta)(\partial \ln B^T/\partial T) - 1] \\ & + [(A^2-1)/A^2](\partial B^s/\partial p)_T \\ & + [(A-1)/A]^2 [1 + (1/\beta)(\partial \ln \beta/\partial T)_p], \end{aligned} \quad (5.17)$$

where $A = C_p/C_v = B^s/B^T = 1 + \beta T \gamma_G$ and for alumina at room-temperature $C = 0.04$. Since $(dB^s/dp)_{T=298^\circ\text{K}} =$

4.19, $\psi_{G(\text{acoustic})} = 4.23$ according to Eq. (5.16); this is in good agreement with $\psi_{G(\text{thermal})} = 4.1$ but it disagrees with 3.6 found for the Lucalox.¹³

It is frequently assumed by some authors³³ that the ratio of specific heats (i.e., C_p/C_v) is unity. The implication of this assumption is that the lattice vibrations of solid under consideration are *harmonic* and that the quantity given by $(\beta T \gamma_G)$ and its temperature dependence is zero. This is a misleading assumption, and because of this assumption inconsistent formalisms are often found in the literature. Aluminum oxide is a relatively incompressible material (thus relatively low expansivity). However, as evident from Table IX, the value of $(\beta T \gamma_G)$ at room temperature is 6.6×10^{-3} and at $T \cong \theta_D$, $(\beta T \gamma_G)$ is 33.4×10^{-3} . At higher temperatures, β and γ_G approach a constant value; thus, the quantity $(\beta T \gamma_G)$ is proportional to temperature. Since $(\beta T \gamma_G)$ is inversely proportional to the lattice thermal conductivity, the high-temperature conductivities of alumina can be understood from the data.

Figure 5 shows a plot of experimental compression points of Bridgman (0–30 kbar)⁹ and also those of Hart and Drickamer (0–300 kbar).¹⁰ Also included are the shock-wave data of McQueen and Marsh¹¹ on both single-crystal (500–1500 kbar) and polycrystalline (300–1300 kbar) aluminas. The lines drawn in the figure are the results of the Murnaghan equation of state²⁴ using the acoustic parameters defined at different boundary conditions. A similar curve to Fig. 5 has been given by Anderson,³⁴ but Anderson used the acoustic parameters derived from the Lucalox material. What is apparent in Fig. 5 is that the Murnaghan parameters evaluated from both the single-crystal and polycrystalline acoustic data give a reasonable description of the pressure-volume relation for the experimental compression points including the shock-wave data. Finally, it may be mentioned that the Murnaghan equation of state and effects of evaluating the Murnaghan parameters at different thermodynamic boundary conditions² can not be seen in the scale of a plot of the kind shown in Fig. 5. Thus, on the basis of this consideration and following Murnaghan,²⁴ the most probable equation of state for alumina is

$$V/V_0 = (1 + 1.653 \times 10^{-3} p)^{-0.2364} \quad (5.18)$$

and this will describe the pressure-volume relation to pressures of a few megabars.

5.3. The Debye Temperature

Values of the Debye temperature as a function of temperature were calculated from the elastic moduli, and these have been tabulated in the last column of Table VII. The low-temperature limit of the Debye

³³ Y. A. Chang, J. Phys. Chem. Solids 28, 697 (1967).

³⁴ O. L. Anderson, J. Phys. Chem. Solids 27, 547 (1966).

³² F. Birch, J. Geophys. Res. 73, 817 (1968).

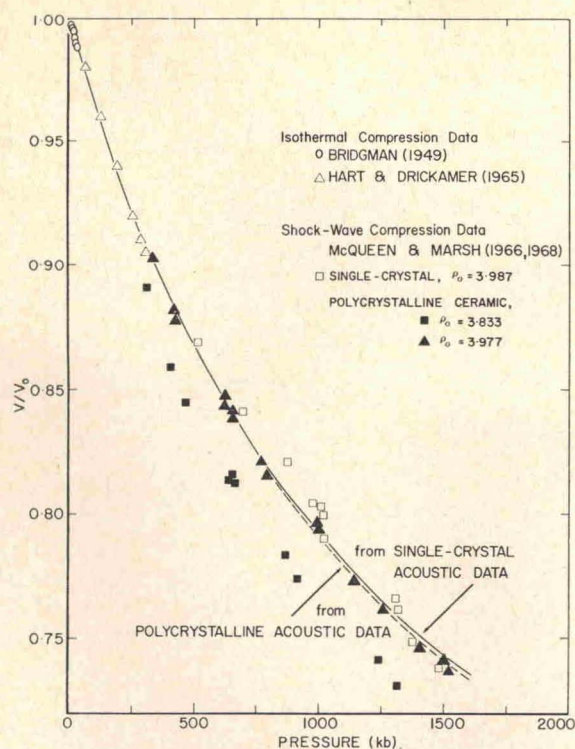


FIG. 5. The compression of single-crystal and polycrystalline alumina.

temperature for alumina was found as $1044(\pm 3)^{\circ}\text{K}$, and it may be noted that this value of the elastic Debye theta agrees very well with thermal Debye theta obtained from the low-temperature specific heat data.⁵ The thermal Debye theta, according to the Barron-Berg-Morrison scheme, is $1045(\pm 6)^{\circ}\text{K}$.⁷

The equivalent values of the Debye temperature of alumina as a function of pressure were also evaluated at the constant temperature of 298°K , and these results have been entered in Table III. It may be noted that a linear increase of about $\frac{1}{2}\%$ in the Debye temperature due to a pressure of 10 kbar is seen here. This increase of the Debye temperature with pressure can be understood by considering the Grüneisen theory of solids in which the frequency of lattice vibrations ν is assumed to be a function only of volume. Thus, we write

$$\nu \sim V^{-\gamma_G},$$

where γ_G is the Grüneisen parameter. Introducing the definition of the Debye temperature and taking the ratio of the theta at a pressure p to that at the reference pressure p_0 , we find that

$$\ln[\Theta_D/\Theta_{D(0)}] = \gamma_G \ln(V_0/V). \quad (5.19)$$

According to this relation, Θ_D increases parabolically with pressure for all the solids of which $(V_0/V) > 1$.

ACKNOWLEDGMENTS

We thank J. H. Gieske for providing his single-crystal data reproduced in Table IV prior to his own publication. R. L. Coble is acknowledged for his most authoritative discussion on Lucalox alumina. This work was started by one of us (DHC) at Materials Research Laboratory of The Pennsylvania State University with support received from U.S. Office of Naval Research Contr. No. Nonr-656(27). The work was completed at Massachusetts Institute of Technology and was supported by National Aeronautics and Space Administration Grant No. NGR-22-009-176.

